CRUSTAL STRUCTURE OF NORTH IRAQ FROM RECEIVER FUNCTION ANALYSES

Roland Gritto[1], Matthew S. Sibol[1], Jacob E. Siegel[1], Hafidh A. Ghalib[1], Youlin Chen[1], Robert B. Herrmann[2], Ghassan I. Alequabi[3], Hrvoje Tkalcic[4], Bakir S. Ali[5], Borhan I. Saleh[5], Dawood S. Mahmood[6,7], Omar K. Shaswar[9,10], Aras Mahmood[5], Shaho Abdullah[5], Fadhil Ibrahim[8], Rashid Zand[8], Basoz Ali[5], Layla Omar[5], Nokhsha I. Aziz[5], Nian H. Ahmed[5], Talal Al-Nasiri[10], Ali A. Ali[7], Abdul-Karem A. Taqi[7], and Samira R. Khalaf[7]

Array Information Technology[1], Saint Louis University[2], Washington University in Saint Louis[3], Australian National University[4], Sulaimaniyah Seismological Observatory[5], Iraq Meteorological Organization[6], Baghdad Seismological Observatory[7], Erbil Seismological Observatory[8], Sulaimaniyah University[9], and University of Baghdad[10]

Sponsored by Air Force Research Laboratory

Contract No. FA8718-07-C-0008
Proposal No. BAA07-59

ABSTRACT

A primary objective of this project is to estimate the local and regional seismic velocity structures of north and northeastern Iraq, including the northern extension of the Zagros collision zone. Furthermore, earthquake source mechanisms will be investigated once a velocity model is derived for this region. Thus far, global seismic network coverage is poor throughout the region and extrapolated velocity models found in the literature lack sufficient accuracy to permit events to be located with significant precision. Ten three-component broadband stations composing the North Iraq Seismographic Network (NISN) were installed in late 2005. At present, waveforms from 290 teleseismic events, from November 30, 2005 through March 31, 2007, have been processed for P-wave receiver functions (RFs). Based on the USGS Preliminary Determination of Epicenters (PDE) bulletins, the epicentral distances of these teleseismic events to NISN stations range from 30º to 90º while their magnitudes equal or exceed 5.5. Results obtained to date indicate a lower-than-average shear wave velocity when compared to other crustal regions of the Earth. Additionally, Moho depths appear slightly shallower below the stations located along the foothills compared to the stations at higher elevation in the Zagros mountains. The Moho below the foothills is estimated at 40-50 km depth, while it dips down to a depth of 45-55 km below the northern extension of the Zagros zone. Common among the receiver functions is the presence of a significant velocity discontinuity at a depth of 15 km and 20 km for the stations below the foothills and Zagros mountains, respectively. The increase in velocity across this discontinuity lead to the observation of mid-crustal refracted body waves throughout NISN. Evaluation of the resulting models will be performed through relocation of recorded events, synthetic waveform analysis, and correlation with available geophysical and geological information.

Report Documentation Page

Form Approved
OMB No. 0704-0188

1. REPORT DATE	2. REPORT TYPE	3. DATES COVERED
SEP 2008		**00-00-2008 to 00-00-2008**

4. TITLE AND SUBTITLE	5a. CONTRACT NUMBER
Crustal Structure of North Iraq from Receiver Function Analyses	5b. GRANT NUMBER
	5c. PROGRAM ELEMENT NUMBER
6. AUTHOR(S)	5d. PROJECT NUMBER
	5e. TASK NUMBER
	5f. WORK UNIT NUMBER
7. PERFORMING ORGANIZATION NAME(S) AND ADDRESS(ES) **Array Information Technology,140 Bessemaur Dr,East Lansing,MI,48823**	8. PERFORMING ORGANIZATION REPORT NUMBER
9. SPONSORING/MONITORING AGENCY NAME(S) AND ADDRESS(ES)	10. SPONSOR/MONITOR'S ACRONYM(S)
	11. SPONSOR/MONITOR'S REPORT NUMBER(S)

12. DISTRIBUTION/AVAILABILITY STATEMENT
Approved for public release; distribution unlimited

13. SUPPLEMENTARY NOTES
Proceedings of the 30th Monitoring Research Review: Ground-Based Nuclear Explosion Monitoring Technologies, 23-25 Sep 2008, Portsmouth, VA sponsored by the National Nuclear Security Administration (NNSA) and the Air Force Research Laboratory (AFRL)

14. ABSTRACT
see report

15. SUBJECT TERMS

16. SECURITY CLASSIFICATION OF:			17. LIMITATION OF ABSTRACT	18. NUMBER OF PAGES	19a. NAME OF RESPONSIBLE PERSON
a. REPORT **unclassified**	b. ABSTRACT **unclassified**	c. THIS PAGE **unclassified**	**Same as Report (SAR)**	**8**	

OBJECTIVE

The objective of the current paper is to estimate the seismic velocity structure beneath the stations of the North Iraq Seismographic Network (NISN) based on RFs inversion techniques. This effort will subsequently be supplemented by the determination of crustal structure from surface wave dispersion analyses. The two methods are complementary and provide valuable constraints on estimating seismic velocity structures. Evaluation of the resulting models will be performed through relocation of recorded events, synthetic waveform analysis, and correlation with available geophysical and geological information.

In November 2005 and in cooperation with the Sulaimaniyah, Erbil, Baghdad, and Mosul seismological observatories (SSO, ESO, BSO and MSO, respectively) the first eight stations of NISN were deployed, followed by stations BHD in Baghdad and MSL in Mosul in April 2006. Figure 1 shows a generalized diagram of the seismotectonic framework of the Arabian plate. NISN stations (white triangles) are located along the northeast boundary of the plate where the Zagros thrust zone and the Bitlis suture zone converge. This region is characterized by a high level of seismic activity, as evidenced by the large number of local and regional events recorded by NISN (Ghalib et al., 2006) and by the teleseismically located earthquakes reported by the United Stated Geological Survey (USGS) bulletins. A close up of the geographic location of NISN is presented in Figure 2. The NISN stations, located parallel to the strike of the Zagros fold belt, are divided in two groups; one along the foothills and the other at higher elevation in the Zagros mountains. Since December 2005, Array IT has collected over 760 GB of data from NISN including local, regional and teleseismic events. The data consist of high-quality, continuous, three-component broadband recordings collected at a rate of 100 sps. Although the seismicity rate of the Zagros fold and thrust zone alone is relatively high, it may have gone mostly undocumented in the past. One explanation is that many of the unreported events are small and may not have been detectable by the regional stations in Turkey and Iran. Second, degradation of Iraq Seismological Network (ISN) capability has significantly impacted monitoring events in this region. Also, noteworthy to mention is that many of the events reported by the USGS and ISC seem to cluster around the local stations in Iran and Turkey that reported their parameters, leaving a major section of the Zagros, its foothills and fold belt to be covered by NISN in an effective and comprehensive manner. The average seismicity rate for local and regional earthquakes recorded by NISN is approximately 150 events per month, resulting in an unprecedented dataset available for research under this effort.

RESEARCH ACCOMPLISHED

RFs are reflection time-series computed from three-component seismograms that represent the relative response of seismic waves to the earth structure near a receiver (Ammon, 2006). The RF methodology has been extensively used by seismologists. While the overall method is straightforward to define, the computation of reliable receiver functions can be problematic due to the non-uniqueness of RF inversions and has been the subject of many studies, including Burdick and Langston (1977), Langston (1977), Ammon (1991), Cassidy (1992), Ligorría and Ammon (1999), Park and Levin (2000), and Helffrich (2006). The current approach is based on the techniques by Zhu and Kanamori (2000), Julià et al. (2000), and Ammon (2006) to determine RFs and invert for crustal seismic velocity models.

A search of the USGS PDE bulletins for the period from 30 November 2005 to 31 March 2007 resulted in a long list of teleseismic events at various azimuths and epicentral distances in the range of 30–90 degrees from NISN. Corresponding searches of NISN for events exceeding magnitude 5.5 resulted in about 290 events available for analysis. The azimuthal distribution of these events relative to NISN is presented in Figure 3. The distribution of events is not symmetric, as most epicenters are located along the western rim of the pacific region from the Aleutian Islands to the north-east to Indonesia to the south-east. In contrast, events to the west are located along the Mid-Atlantic ridge, while events to the south are grouped along the Southwest Indian Ridge and the East-African Rift Zone. The variation of RFs at each station with respect to azimuth and ray parameter of the incoming waves was investigated. It was found, however, that this variation is not very significant.

An example of teleseismic waveform data recorded at stations KSBB, KSSS, and KSWW is shown in Figure 4. The event occurred in the Kuril Islands on 22 June 2006 with a magnitude (Mw) of 6.0. The quality of observed P-waves was assigned a grading scale (A, good, through D, poor) to reflect the minimum signal-to-noise level

which still produced stable and reliable receiver functions. The grading helped to understand the impact of signals with low signal-to-noise ratios on the RFs and resulting models. In the final data processing, only good-quality waveforms (grade A and B) were used.

In order to fit the observed RFs we use an iterative linearized inversion technique (Ammon, 2006), which strongly depends on the starting model. The best starting model is estimated using the method by Zhu and Kanmori (2000), which generates a three-layered model over a half space providing an initial Moho depth and v_p/v_s-ratio beneath each station. The result of the initial search is presented in Table 1.

Table 1: Summary of initial search results for Moho depth and v_p/v_s-ratio beneath the stations of NISN

Station	Available events	Used events	Moho Depth [km]	v_p/v_s
KDDA	112	29	52.3+/-0.8	1.62+/-0.05
KEHH	127	55	49.8+/-1.4	1.55+/-0.06
KEKZ	131	15	44.7+/-0.8	1.80+/-0.06
KESM	94	46	39.1+/-0.9	1.83+/-0.07
KSBB	136	42	48.6+/-1.3	1.70+/-0.06
KSJS	123	32	48.9+/-1.2	1.73+/-0.08
KSSS	103	53	52.3+/-0.8	1.85+/-0.05
KSWW	134	65	54.2+/-0.7	1.71+/-0.06

A cross correlation approach was subsequently used to determine the most coherent RFs at each station before they were stacked to generate the final observed RF.

In preparation for the inversion process, the Moho depths and v_p/v_s-ratio obtained from Table 1 were used to generate a simple multi-layered initial compressional- and shear-velocity model which followed the general characteristics of the models derived by Ghalib (1992). The thicknesses of the crustal layers varied from 0.5 km at the top to a maximum of 10 km at the bottom, representing a gradual increase with depth. In the upper mantle, the layer thicknesses ranged from 10 to 100 km.

The resulting one-dimensional shear-wave velocity models for stations KESM, KEHH, KSWW, KSSS, KDDA, KEKZ, KSJS, and KSBB are presented in Figure 5. The best fit of these RFs ranged from 60% to 93%, while the back-azimuth to these events ranged from 20 to 120 degrees. Common among the eight models are the relatively low shear-wave velocities of the layers in comparison to other regions of the Earth and the presence of a significant positive velocity discontinuity between upper and lower crust. The results of the RF inversion suggest a slightly shallower Moho below the foothills at 40-50 km depth, while it dips down to 45-55 km below the Zagros mountains. All crustal models indicate the presence of a significant positive velocity discontinuity at about 15 km and 20 km depth for the stations below the foothills and Zagros mountains, respectively. The increase in velocity across this discontinuity resulted in the observation of mid-crustal refracted body waves throughout NISN. These results are consistent with previous observations made by, among others, Aleqabi et al. (2007), Pasyanos et al. (2004), and Ghalib (1992).

CONCLUSIONS AND RECOMMENDATIONS

The presented results are part of an ongoing effort to estimate the seismic velocity structure beneath eight of the NISN three-component broadband stations. The presented models were exclusively estimated from the inversion of PFs of teleseismic P wave seismograms. Most significant about these models is that they consistently reflect lower-than-average velocities, as has previously been observed, which seems to characterize the crustal structure of this region.

Continuous data collection and processing of teleseismic P- and surface-wave data is currently under way for refinement of the presented results and simultaneous inversion. These data will help generate more-reliable models

that can withstand the test of relocating events with higher precision and synthetic waveform modeling that matches well with the observed seismograms.

ACKNOWLEDGEMENTS

The figures and maps throughout this document were created using the Generic Mapping Tools by Wessel and Smith (1998).

REFERENCES

Aleqabi, G., M. Wysession, H. A. A. Ghalib, M. Sibol, B. Saeed Ali, B. Saleh, A. Mahmood, S. Abdullah, L. Omar, N. Aziz, N. Ahmed, D. Mahmood, N. Alridaha, T. Alnasiry, O. Shaswar, A. Ali, A. Taqi, S. Khalaf, and F. Ibrahim (2007). Seismic velocity structure of Iraq and surrounding regions from surface-waves waveform inversion, *Seism. Res. Lett.* 78: 310**.**

Julià, J., C. J. Ammon, R.B. Herrmann, and A. M. Correig (2000). Joint inversion of receiver function and surface wave dispersion observations, *Geophys. J. Int.* 143: 1-19.

Zhu, L. and H. Kanamori (2000). Moho depth variation in southern California from teleseismic receiver functions, *J. Geophys. Res.* 105: 2969–2980.

Ammon, C. J. (1991). The isolation of receiver effects from teleseismic P waveforms, *Bull. Seism. Soc. Am.* 81: 2504–2510.

Ammon, C. J. (2006). Receiver-Function Analysis, Pennsylvania State University, Web page: http://eqseis.geosc.psu.edu/~cammon/HTML/RftnDocs/rftn01.html

Burdick, L. J. and C. A. Langston, (1977). Modeling crustal structure through the use of converted phases in teleseismic body-wave forms, *Bull. Seism. Soc. Am.* 67: 677–691.

Cassidy, J. F. (1992). Numerical experiments in broadband receiver function analysis, *Bull. Seism. Soc. Am.* 82: 1453–1474.

Ghalib, H. A. A., G. I. Aleqabi, B. S. Ali, B. I. Saleh, D. S. Mahmood, I. N. Gupta. R. A. Wagner, P. J. Shore, A. Mahmood, S. Abdullah, O. K. Shaswar, F. Ibrahim, B. Ali, L. Omar, N. I. Aziz, N. H. Ahmed, A. A. Ali, A.-K. A. Taqi, and S. R. Khalaf (2006). Seismic characteristics of northern Iraq and surrounding regions, in *Proceedings of the 28th Seismic Research Review: Ground-Based Nuclear Explosion Monitoring Technologies*, LA-UR-06-5471, Vol. 1, pp. 40–48.

Ghalib, H. A. A. (1992). Seismic velocity and attenuation of the Arabian plate, Ph.D. dissertation, Saint Louis University, 1–314.

Helffrich, G. (2006). Extended-time multitaper frequency domain cross-correlation receiver-function estimation, *Bull. Seism. Soc. Am.* 96: 344–34.

Langston, C. A. (1977). The effect of planar dipping structure on source and receiver responses for constant ray parameter, *Bull. Seism. Soc. Am.* 67: 1029–1050.

Ligorría, J. P. and C. J. Ammon (1999). Iterative deconvolution and receiver-function estimation, *Bull. Seism. Soc. Am.* 89: 1395–1400.

Park, J. and V. Levin (2000). Receiver functions from multiple-taper spectral correlation estimates, *Bull. Seism. Soc. Am*. 90: 1507–1520.

Pasyanos, M. E., W. R. Walter, M. Flanagan, P. Goldstein, and J. Bhattacharyya (2004). Building and testing a priori geophysical model for western Eurasia and North Africa, *Pure Appl. Geophys*. 161: 235–281.

Wessel, P. and W. H. F. Smith (1998). New, improved version of Generic Mapping Tools released, *EOS, Trans. AGU* 79: 579.

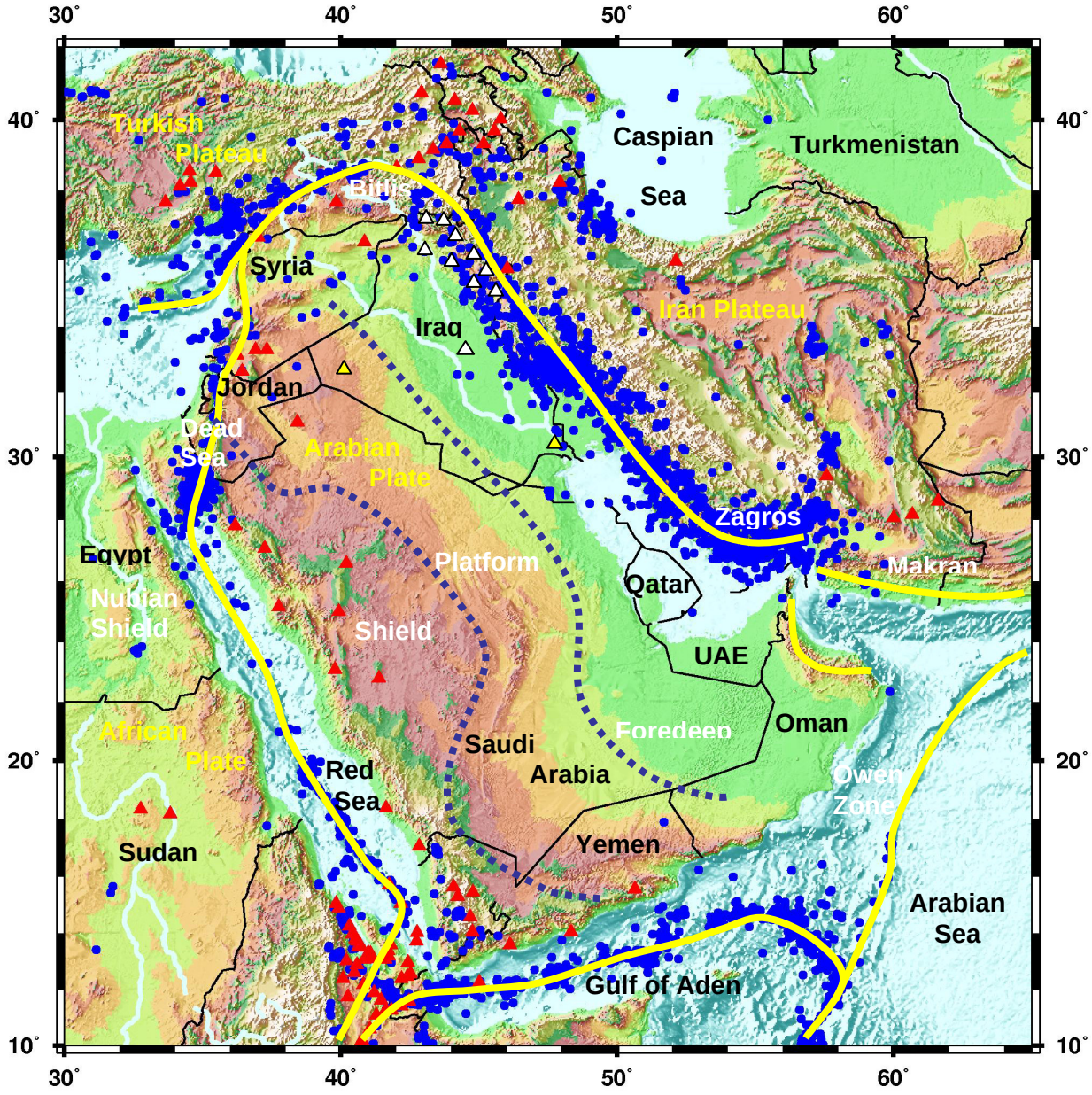

Figure 1: Map of the Arabian Peninsula and surrounding regions. The major geographic, tectonic and geologic features are labeled. The plate boundaries are marked with yellow lines. Earthquakes and volcanoes are shown as blue circles and red triangles, respectively. White triangles represent the 10 stations that comprise North Iraq Seismological Network (NISN). The yellow triangles reflect the location of some of Iraq Seismological Network (ISN), but are currently not operational.

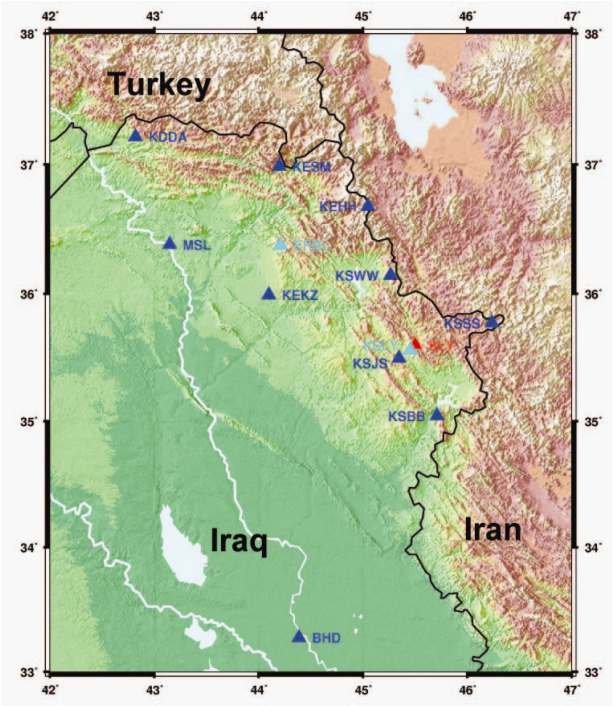

Figure 2. Geographic location of the North Iraq Seismic Network (NISN). Ten PASSCAL stations (blue triangles) are currently operational throughout north-eastern Iraq. Light blue triangles indicate temporary sites of two stations (ERBL and KSLY). The red triangle (SLY) signifies the original location of one of Iraq Seismological Network (ISN) original five stations.

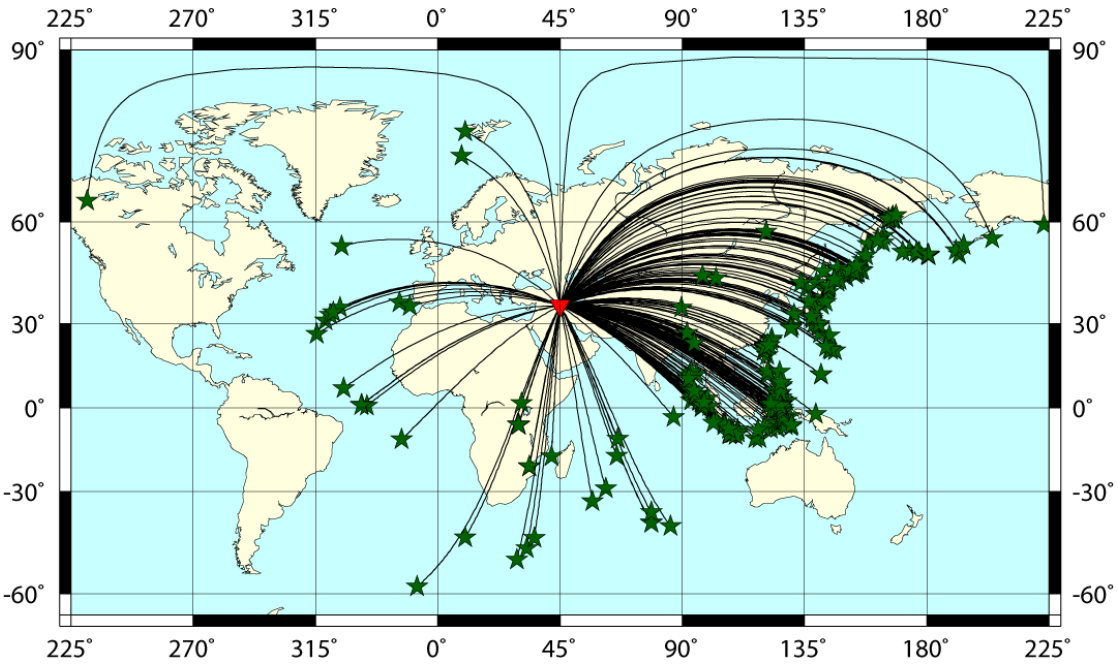

Figure 3. Global distribution of events (Mb > 5.5, from November 2005 to March 2007). Green stars denote earthquake epicenters, black lines the great-circle paths of the waves from the events to the network and the red triangle the location of NISN.

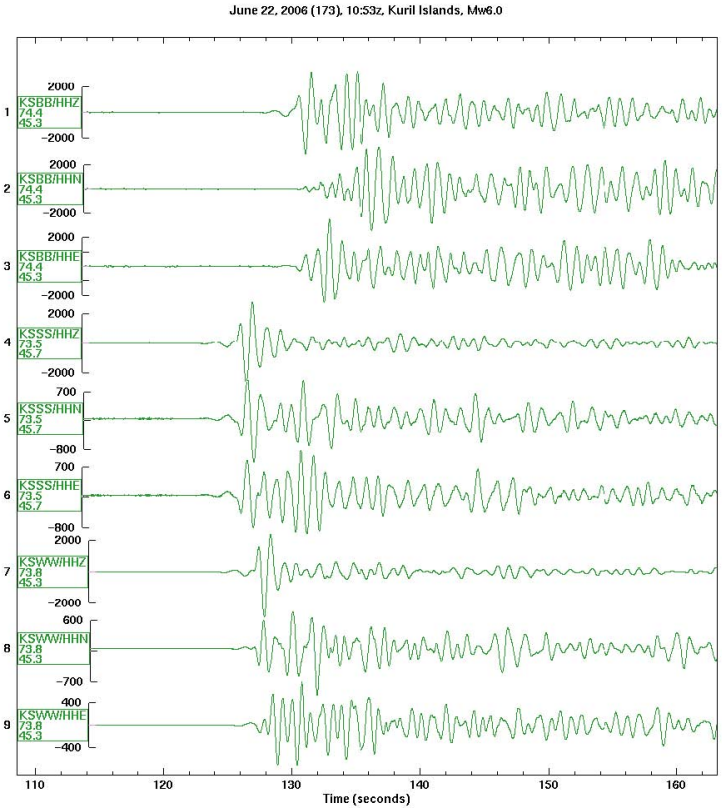

Figure 4. Broad-band seismogram records of teleseismic P-waves of a Mw 6.0 event located in the Kuril Islands. Waveforms were recorded at three NISN stations (KSBB, KSSS, and KSWW) and subsequently used in RF inversion.

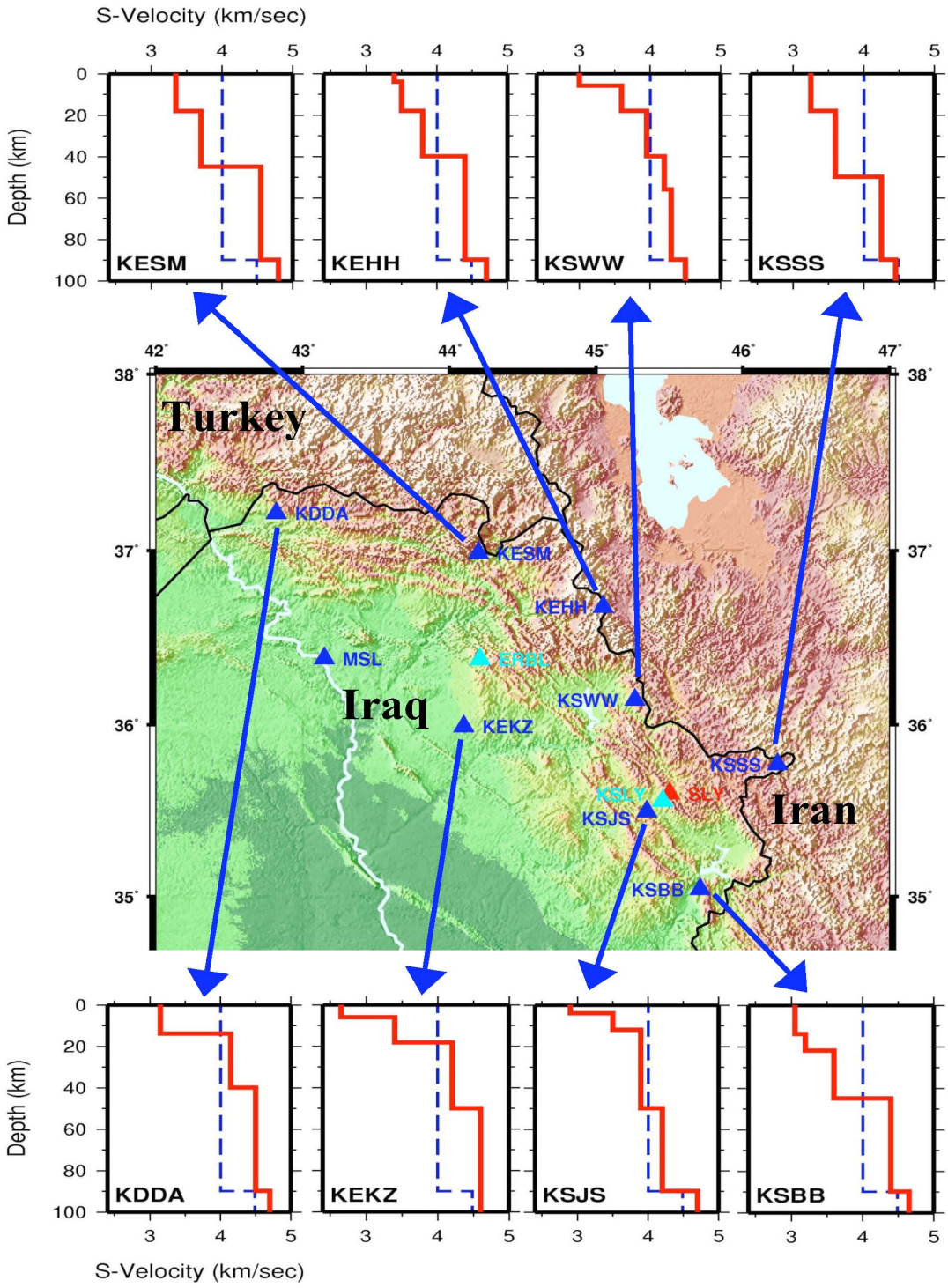

Figure 5. **Locations of NISN stations (blue triangles) and associated shear-wave velocity models obtained from RF inversion. Moho depths beneath the stations in the foothills appear shallower than those beneath the stations in the Zagros mountains. Similarly, a mid-crustal velocity increase appears at shallower depth below the foothills (~ 15 km depth) compared to the Zagros mountains (~ 20 km depth). Station ERBL and KSLY (aqua triangles) are the temporary stations. Station SLY (red triangle) belongs to ISN.**